Supplementary

S1. Patient-based aneurysm models

The patient-specific vascular lumen was segmented from a clinical 3D rotational angiographic dataset (3D RA) of a patient with a basilar bifurcation tip aneurysm. To simplify the experimental setup, the distal branches were cut approximately 3 cm distally from the aneurysm neck, and the superior cerebellar arteries were combined with the posterior cerebral arteries (Fig. S1 top left). Next, the patient-specific aneurysm sac was removed and five artificial aneurysm sacs with dimensions of the aneurysm neck ranging from 2.7 to 9.7 mm were combined with the vessel lumen (Fusion 360 2.0, Autodesk, USA). The artificial aneurysms were wide-necked bifurcation aneurysms with a comparable dome-to-neck ratio (1.2±0.1). Contours sized 5, 11, and 14 mm are suitable for the resulting aneurysm based on the manufacturer's recommendations (Table S1). The models were then completed by adding an outer layer to form a vessel wall, and 3D printed (Clear Photoreactive Resin, Form 3, Formlabs, USA).

Table S1. First-generation contour neurovascular contour devices (contour): sizes and corresponding recommendations for the aneurysm sizes (Cerus Endovascular, Instructions: www.cerusendo.com/contour-neurovascular-system).

Contour Diameter (mm)	Aneurysm Neck (mm)	Aneurysm width (mm)
5	2.0 – 3.0	2.0 – 3.5
7	3.0 – 5.0	3.0 – 5.5
9	4.0 – 6.0	5.0 – 7.5
11	5.0 – 8.0	7.0 – 8.5
14	7.0 – 10.0	8.0 – 10.5

Table S2. Comparison of treatment effect (TE) without and with SCA branches for chosen hemodynamic parameters of case A3 C6.

A3 C6	TE of NIR	TE of AWSS	TE of V	TE of KE	TE of ICI	TE of OVI	TE of OSI
Without SCAs	-57%	-78%	-59%	-86%	-54%	-83%	-77%
With SCAs	-55%	-76%	-57%	-85%	-52%	-78%	-77%

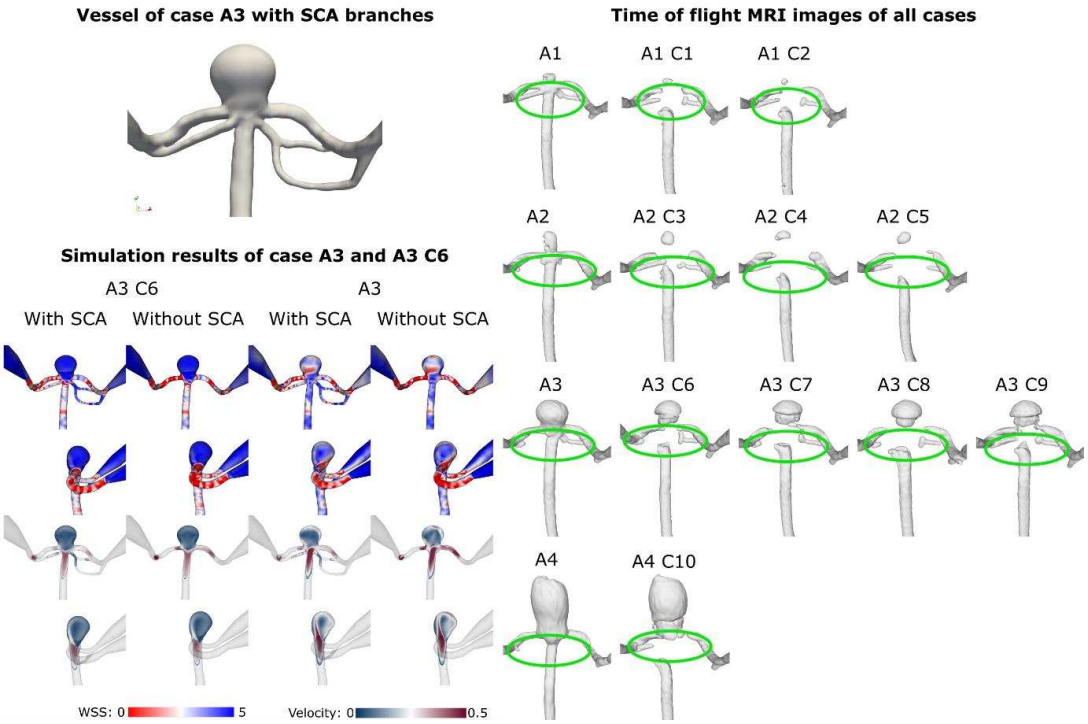

Figure S1: Top left: Vessel A2 used for 3D-printing. Bottom left: Comparison of qualitative velocity and wall shear stress patterns in A3 and A3 C6 with and without SCA vessels included. Right: Vascular segmentation from TOF MRI data of all models without (A1-A4) and with (C1-C10) Contour implanted. Notice the occluded SCA branches in most of the cases due to insufficient 3D printing (marked with green circles).

S2. Flow Setup and In Vitro Device Deployment

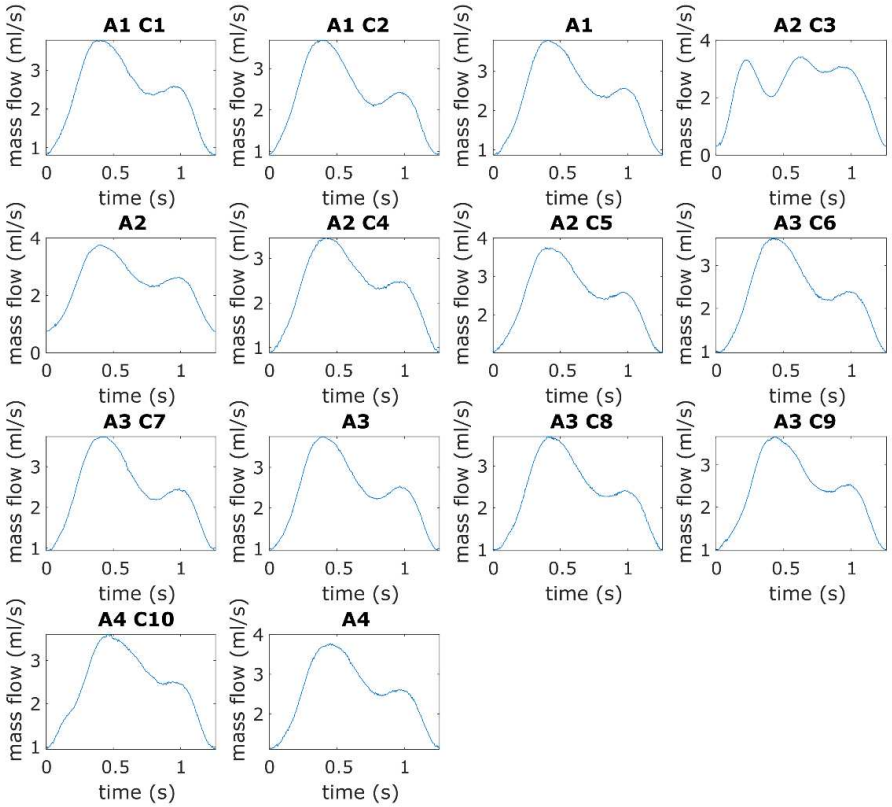

Figure S2: Mass flow curves set as boundary conditions at the inlet for each case A1-A4 and C1-C10.

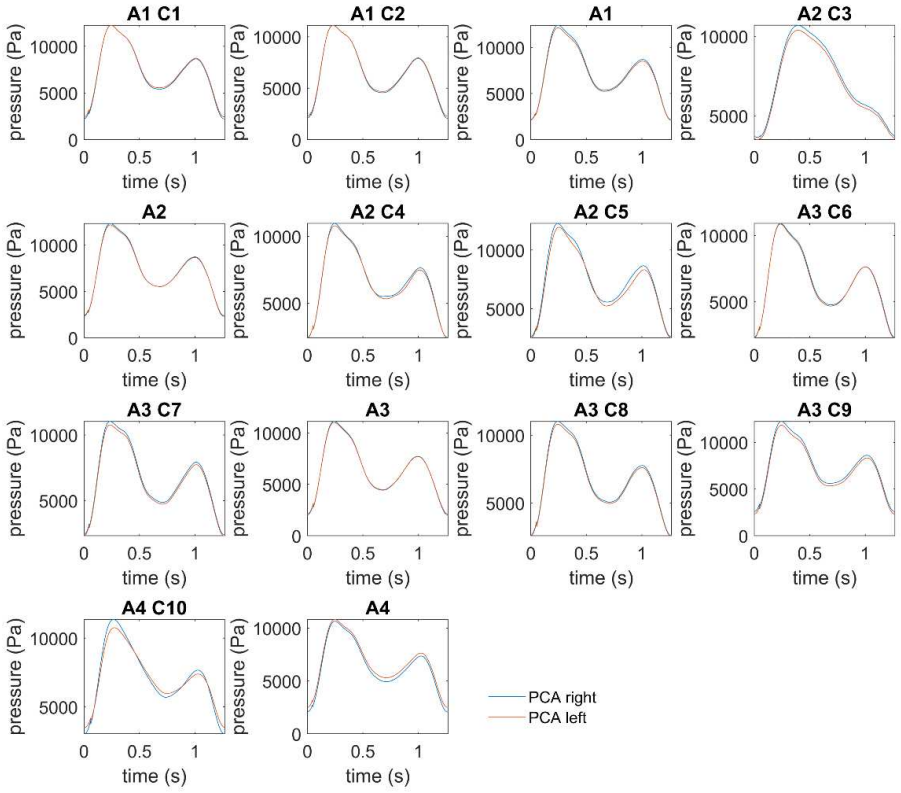

Figure S3: Pressure curves set as outlet boundary conditions for each case A1-A4 and C1-C10.

For implantation, an intermediate catheter was employed (Navien 0.072'', Medtronic, Minneapolis, MN, USA) and a microcatheter (Phenom 0.027'', Medtronic, Minneapolis, MN, USA) navigated into the center of the sac of the aneurysm model. Then, the devices were placed in the neck of the aneurysm and detached electrolytically after mechanical stability was confirmed. Angiographic contrast stasis was observed after the placement of each device indicating flow reduction at the aneurysm.

S3. Magnetic Resonance imaging

The 4D flow MRI was performed using a 3D T1-weighted spoiled fast gradient echo sequence with Cartesian sampling (echo time/repetition time: 5/8.5 msec; field of view: $110 \times 110 \times 40$ mm^3; voxel size: (0.75 mm)^3; flip angle: 8°). The sequence was accelerated 4.5-fold with a compressed-sensing technique implemented by the vendor (Philips); the examination time was 41.4 minutes. For velocity encoding, a balanced symmetric 4-point phase-contrast encoding scheme (Hadamard) was used. An integrated artificial digital trigger was used for temporally resolved data acquisition, and 20 cardiac phases were obtained. The velocity-encoding parameter was set to 75 cm/s for all experiments. The velocity noise was less than 5 cm/s. The velocity noise was estimated by calculating velocity values at the static region (outside of the flow volume) in center of the imaging volume for model A4-C10.

S4. Virtual Processing Pipeline

Table S3: Quantitative comparison of geometric parameters after the deformation using the processing pipeline. RPM: Radiopaque marker. The values are averaged for the respected Contour devices (5,11,14 mm)

Geo. parameter	CN05			CN11			CN14		
	CAD	µCT	Diff [%]	CAD	µCT	Diff [%]	CAD	µCT	Diff [%]
Total length [mm]	3.63	3.7	1.89	6.49	6.99	7.21	8	8.78	8.88
Diameter average [mm]	2.5	2.53	1.19	7.15	7.16	0.14	8,56	8.76	2.28
Average grid thickness [mm]	0.02	0.07	71.43	0.02	0.08	75	0.022	0.09	75.56
Total Volume [mm³]	9.22	10.78	14.47	135.44	140.09	3.32	325.66	330.82	1.55
Total Area [mm²]	26.79	28.03	4.42	151.03	155	2.56	254.16	256.07	0.75

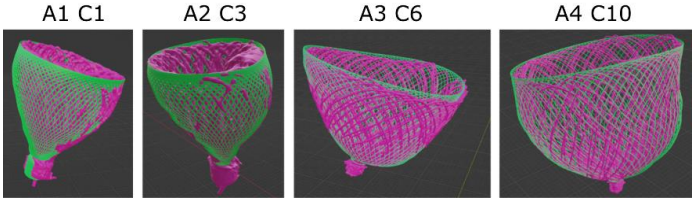

Figure S4: Visual representation of the Contour fit between virtually deformed CAD Contour (green) and µCT (pink) for four cases.

S5. Hemodynamic parameters

Oscillatory Shear Index (-): $$OSI = \frac{1}{2}\left\{1 - \frac{\frac{1}{T}\left|\int_0^T WSS\, dt\right|}{\frac{1}{T}\int_0^T |WSS| dt}\right\}$$

Oscillatory Velocity Index (-): $$OVI = \frac{1}{2} * \left\{1 - \frac{\frac{1}{T}\left|\int_0^T V\, dt\right|}{\frac{1}{T}\int_0^T |V| dt}\right\}$$

Time-averaged Wall Shear Stress (Pa): $$TAWSS = \frac{1}{T}\int_0^T |WSS| dt$$

Kinetic Energy (J): $$E_{kin} = \frac{1}{2} * \rho V^2$$

Inflow Concentration Index (-): $$ICI = \frac{Q_{inflow}/Q_{parentvessel}}{A_{inflow}/A_{ostium}}$$

Aneurysm turnover time (s): $$TOT = \frac{Volume_{IA\,sac}}{Neck\ inflow\ rate}$$

S6. Results

Table S4: Detailed information about the treatment effect (%) for each case C1-10 compared to the models without Contour (A1-4) for specific hemodynamic parameters (underlying information for Figure 4a)

Contour	NIR	AWSS	V	KE	ICI	OVI	OSI
A1 C1	-0.86	-0.90	-0.88	-0.98	-0.96	-0.54	-0.60
A1 C2	-0.99	-1.00	-1.00	-1.00	-0.99	0.06	0.06
A2 C3	-0.89	-0.98	-0.96	-1.00	-0.91	-0.64	-0.29
A2 C 4	-0.84	-0.96	-0.91	-0.98	-0.96	-0.68	-0.53
A2 C 5	-0.88	-0.95	-0.96	-0.99	-0.97	1.16	1.26
A3 C6	-0.57	-0.78	-0.59	-0.86	-0.54	-0.83	-0.77
A3 C 7	-0.70	-0.87	-0.76	-0.95	-0.59	-0.78	-0.70
A3 C 8	-0.65	-0.84	-0.69	-0.93	-0.61	-0.85	-0.69
A3 C 9	-0.71	-0.87	-0.73	-0.94	-0.49	-0.65	-0.57
A4 C10	-0.47	-0.87	-1.00	-0.94	-0.34	0.16	-0.04

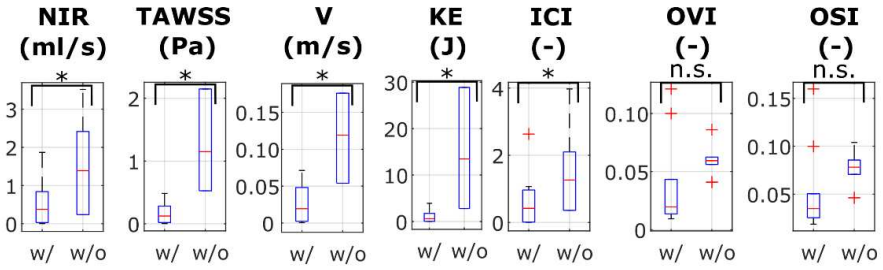

Figure S5: Boxplots comparing hemodynamic parameters between with (w/) and without (w/o) Contour. Significant differences are marked with a '*'

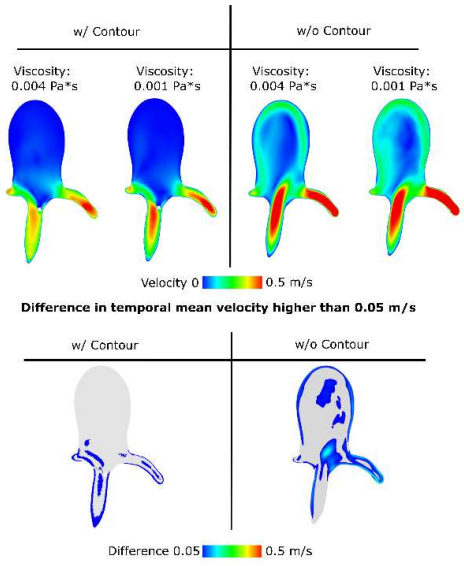

Figure S6: Comparison of the resulting velocities from CFD simulation of case A4 and A4 C10 with different viscosities (blood: 0.004 Pa*s and water: 0.001 Pa*s) and the visualization of the absolute difference in velocity higher than 0.05 m/s.